AJNR

MR angiography of ruptured aneurysms in acute subarachnoid hemorrhage.

M Ida, Y Kurisu and M Yamashita

AJNR Am J Neuroradiol 1997, 18 (6) 1025-1032
http://www.ajnr.org/content/18/6/1025

MR Angiography of Ruptured Aneurysms in Acute Subarachnoid Hemorrhage

Masahiro Ida, Yasuhisa Kurisu, and Miyoko Yamashita

PURPOSE: To determine the efficacy of high-resolution MR angiography for the prospective diagnosis of ruptured aneurysms in acute subarachnoid hemorrhage. **METHODS:** We used 3-D time-of-flight MR angiography with a large image matrix (193 × 512 frequency-encoding steps), magnetization transfer saturation, and a variable flip-angle excitation (tilted optimized nonsaturating excitation [TONE]) to study 28 patients with acute subarachnoid hemorrhage. The MR angiograms were compared with intraarterial digital subtraction angiographic (IA-DSA) images. **RESULTS:** Thirty-five (90%) of 39 aneurysms were detected prospectively with MR angiography. At least one aneurysm was identified with MR angiography in 25 (96%) of 26 patients with aneurysms proved by IA-DSA. Although four aneurysms were missed prospectively, three of these were detected retrospectively with MR angiography. Six aneurysms (18%) of those evident on MR angiograms were 3 mm or less in diameter. In one patient, additional targeted maximum intensity projections were greatly helpful for the ensuing IA-DSA by determining the optimizal projection angle by which to depict a ruptured aneurysm that neither routine MR angiography nor routine IA-DSA detected. **CONCLUSION:** High-resolution MR angiography may be a useful diagnostic technique for detecting ruptured aneurysms, even in patients with acute subarachnoid hemorrhage. Initial MR angiography offers valuable and reliable information on ruptured aneurysms in acute subarachnoid hemorrhage, allowing the optimization of projection angles at conventional angiography.

Index terms: Aneurysm, magnetic resonance; Magnetic resonance angiography; Subarachnoid space, hemorrhage

AJNR Am J Neuroradiol 18:1025–1032, June 1997

The three-dimensional time-of-flight (TOF) sequence for intracranial magnetic resonance (MR) angiography has been substantially improved and optimized by the introduction of larger imaging matrices (512 frequency-encoding steps) and magnetization transfer saturation (MTS) and tilted optimized nonsaturating excitation (TONE) techniques. A larger matrix allows a smaller voxel size and decreases phase dispersion. MTS is a background-signal suppression technique that uses an off-resonance radio-frequency pulse to saturate protons in the bound water of the brain parenchyma. MTS enhances contrast between arteries and brain parenchyma. TONE is a variable flip-angle excitation technique to compensate progressive saturation of spins traveling through an imaged volume. The flip angle is set lower at the entry side of an imaged volume and gradually increases as it approaches the exit side, increasing signal intensity in the distal arteries and homogenizing overall vessel intensity. Several authors have described the clinical uses of these improved MR angiographic techniques (1, 2).

At our hospital, 3-D TOF high-resolution MR angiography has been included in the routine MR evaluation of various intracranial diseases. We performed intracranial MR angiography in 3474 patients between October 1994 and April 1996, including 28 patients with acute subarachnoid hemorrhage. Our purpose was to

Received July 5, 1996; accepted after revision January 7, 1997.

Presented at the annual meeting of the American Society of Neuroradiology, Seattle, Wash, June 1996.

From the Department of Radiology, Tokyo (Japan) Metropolitan Ebara Hospital.

Address reprint requests to Masahiro Ida, MD, Department of Radiology, Tokyo Metropolitan Ebara Hospital, 4-5-10, Higashi-Yukigaya, Ootaku, Tokyo 145, Japan.

AJNR 18:1025–1032, Jun 1997 0195-6108/97/1806–1025

evaluate the uses and limitations of high-resolution MR angiography with MTS and TONE in the diagnosis of ruptured aneurysms in the setting of acute subarachnoid hemorrhage.

Subjects and Methods

We performed emergency intracranial MR angiography in 28 patients with acute subarachnoid hemorrhage from October 1994 through April 1996 (seven men and 21 women; 14 to 75 years old; mean age, 53 years). One patient (case 10) had renal dysfunction and another (case 19) had a history of acute febrile mucocutaneous lymph-node syndrome. The initial clinical status of all the patients was graded according to Hunt and Kosnik criteria (3). No patients had grade 0 or 1 disease, 18 patients had grade 2 criteria, six had grade 3 findings, three had grade 4 disease, and one patient was judged to have a clinical status of grade 5. The diagnosis of acute subarachnoid hemorrhage was made on the basis of findings on noncontrast computed tomographic (CT) scans obtained before MR imaging was performed. Severity of hemorrhage at the ruptured aneurysm site on the initial CT scan was categorized as slight (thin hemorrhage in the subarachnoid space around the ruptured aneurysm), moderate (thick hemorrhage without intraparenchymal hematoma), or severe (thick hemorrhage with complicated intraparenchymal hematoma).

Twenty-two patients with a total of 27 aneurysms underwent clipping of the aneurysms. One patient had coil embolization in the chronic stage (case 24). Five patients have been watched conservatively (cases 1, 10, 26, 27, and 28). All MR and conventional angiographic studies were preceded by the procurement of informed consent by the patients and/or their relatives.

MR Angiography

MR angiography was performed within 24 hours (day 1) after the onset of subarachnoid hemorrhage in 27 patients and within 48 hours (day 2) in one patient. A 1.5-T system with 25 mT/m gradient strength was used, with a circularly polarized head coil. Three-dimensional TOF sequences were acquired with fast imaging with steady-state precession (FISP). Imaging parameters were 39/7 (repetition time/echo time), a flip angle of 20° (with TONE), a 210-mm field of view, and a matrix size of 193 × 512 (0.82 mm × 0.41 mm). The section thickness was 70 mm with 70 partitions (the effective section thickness was 1 mm). A gaussian prepulse was added for MTS. The acquisition time was 8 minutes, 49 seconds. The imaged volume for MR angiography was selected to cover both the circle of Willis and the region of the ruptured aneurysm suggested on the preceding CT study.

Multiple stereoscopic MR angiograms were reconstructed immediately after data acquisition by a maximum intensity projection (MIP) algorithm. Orbital fat and venous sinuses were excluded from the region of interest as much as possible. A total of 24 MIP images consisting of 12 images with 10° increments about the anteroposterior axis and 12 images with 10° increments about the head-to-foot axis were created. Targeted MIP images focused on the expected or suspicious location were added to reduce background signals and to avoid overlap of vessels. When necessary, source images (individual partitions) were also used. The time required to prepare the patient, acquire the data, calculate the raw data, and to perform the routine MIP algorithm was approximately 20 minutes.

Intraarterial Digital Subtraction Angiography

Intraarterial digital subtraction angiography (IA-DSA) was performed by femoral artery catheterization and a digital subtraction angiographic system (Multistar Top and Polytron, Siemens, Germany). In 26 patients, IA-DSA was carried out between days 1 and 3; in one patient, it was done on day 6. The remaining patient (case 10) did not undergo IA-DSA in the acute stage because of renal dysfunction; instead, it was performed on day 21 after hydration and diuresis. IA-DSA followed MR angiography in 23 patients and preceded the angiographic study in five patients (cases 1, 14, 16, 23, and 24). Neurosurgeons were provided with the results of the CT and MR angiographic examinations before IA-DSA was carried out. Routine IA-DSA included anteroposterior Towne and lateral views of both internal carotid arteries and the vertebrobasilar arteries, plus bilateral oblique views of the vessel(s) of interest. Various oblique and/or submentovertex views optimal for depiction of the aneurysm were additionally obtained, depending on the results of MR angiography.

Data Analysis

MR angiograms (ie, 24 routine MIP images, targeted MIP images, and source images) were read on an emergency basis by one or two radiologists who had been informed of the initial CT results, including the sites of subarachnoid hemorrhage and degree of hemorrhage. They used both workstation displays and hard copy images. The presence of aneurysms or other vascular disorders, the maximum diameter of the aneurysm, its site, and the parent artery were analyzed. The quality of the MR angiograms was graded as excellent (good quality with no artifacts), fair (slightly noisy but adequate for detecting ruptured aneurysms), or poor (too many artifacts to make an evaluation). IA-DSAs were evaluated by an angiographer (radiologist) who specializes in radiology of vascular diseases. In evaluating the studies of the patients who underwent IA-DSA prior to MR angiography, the readers were blinded to the results of IA-DSA.

Results

The clinical information and MR angiographic and IA-DSA findings in the 28 patients with acute subarachnoid hemorrhage are summa-

Clinical data and results in 28 patients

Patient	Age, y/Sex	Clinical Status, Grade	Degree of Hemorrhage	Prospective Reading of MR Angiography			IA-DSA Findings	Treatment
				Day	Aneurysm Location	Size, mm		
1	39/F	2	Moderate	1*	IC	2	+	ND
2	54/M	4	Moderate	1	IC	7	+	Clipping
3	31/F	2	Moderate	1	IC-PC	3	+	Clipping
					IC-OP	1	+ (unruptured)	ND
4	46/M	2	Moderate	1	IC-PC	4	+	Clipping
5	63/F	2	Moderate	1	IC-PC	2†	+	Clipping
6	32/F	3	Moderate	1	IC-PC	5	+	Clipping
7	42/F	4	Severe	1	IC-PC	4	+	Clipping
8	63/F	2	Moderate	1	IC-PC	10	+	Clipping
					IC-PC	5	+ (unruptured)	ND
9	73/F	2	Moderate	1	IC-PC	12	+	Clipping
					AC	6	+ (unruptured)	ND
10	62/F	2	Moderate	1	IC	7	+	ND
11	49/M	2	Moderate	1	IC-PC (L)	12	+	Clipping
					IC-OP (L)	4	+ (unruptured)	ND
					IC-PC (R)	5	+ (unruptured)	Clipping
					IC-OP (R)	7	+ (unruptured)	Clipping
12	62/M	3	Moderate	1	AC	2	+	Clipping
					MCA	4	+ (unruptured)	ND
13	74/F	2	Moderate	1	AC	4	+	Clipping
					MCA	6	+ (unruptured)	ND
14	52/F	2	Slight	2*	ACA	5	+	Clipping
					MCA	6	+ (unruptured)	Clipping
15	62/F	2	Moderate	1	ACA (L)	4	+	Clipping
					MCA (R)	2	+ (unruptured)	Clipping
16	51/F	3	Slight	1*	MCA	8	+	Clipping
17	59/F	2	Moderate	1	MCA	12	+	Clipping
18	40/M	2	Severe	1	MCA	12	+	Clipping
19	14/M	4	Severe	1	MCA	12	+	Clipping
20	48/M	2	Moderate	1	MCA	5	+ (unruptured)	Clipping
					(not detected)‡		+ AC, 2 mm	Clipping
21	56/F	2	Moderate	1	MCA	5†	+	Clipping
					(not detected)‡		+ IC-PC, 2 mm (unruptured)	ND
22	65/F	2	Moderate	1	MCA (R)	5	+	Clipping
					(not detected)‡		+ MCA (L), 3 mm (unruptured)	ND
23	58/F	3	Severe	1*	MCA	4	+	Clipping
24	63/F	3	Moderate	1*	VA-PICA	5	+	Coiling
25	61/F	3	Moderate	1	VA-PICA	5	+	Clipping
26	75/F	5	Slight	1	(Not detected)§	. . .	+ AICA distal, 3 mm	ND
27	29/F	2	Slight	1	Moyamoya disease	. . .	− Moyamoya disease	ND
28	57/F	2	Severe	1	(Not detected)	. . .	− No aneurysm	ND

Note.—IA-DSA indicates intraarterial digital subtraction angiography; IC, internal carotid artery; PC, posterior communicating artery; OP, ophthalmic artery; AC, anterior communicating artery; ACA, anterior cerebral artery; MCA, middle cerebral artery; VA, vertebral artery; +, IA-DSA showed an aneurysm; −, IA-DSA showed no aneurysm; and ND, not done.

* IA-DSA was carried out before MR angiography; readers of the MR angiograms were blinded to the results of IA-DSA.

† Aneurysm was underestimated in size with MR angiography owing to partial reduction of flow signal.

‡ Aneurysm could be pointed out retrospectively at MR angiography.

§ No aneurysm was detected, even retrospectively, at MR angiography.

rized in the Table. There was no patient who worsened or rehemorrhaged from the aneurysm during or immediately after the MR examination. In 27 of 28 patients, "excellent" MR angiograms were obtained without motion artifacts or excessive background signal from hemorrhage. In one patient with severe subarachnoid hemorrhage (case 21), MR angiograms were impaired slightly by patient motion; however, the quality was sufficient to detect a ruptured aneurysm.

In 25 of 28 patients, 35 aneurysms (16 in the internal carotid artery, two in the anterior cerebral artery, three in the anterior communicating artery, 12 in the middle cerebral artery, and two in the vertebral artery) were identified with MR angiography (Fig 1). In one patient (case 27), MR angiography showed moyamoya disease without a saccular aneurysm. In the remaining two patients (cases 26 and 28), MR angiographic results were initially considered normal. IA-DSA revealed 39 aneurysms in 26 patients, moyamoya disease without a saccular aneurysm in one patient (case 27), and no abnormal findings in one patient (case 28). Even through MR readers prospectively failed to identify four aneurysms in four patients (cases 20, 21, 22, and 26), three of these were detected retrospectively (cases 20–22). These three were unruptured aneurysms in the patients with multiple aneurysms. Six (18%) of the aneurysms shown by MR angiography were 3 mm or less in diameter. Two aneurysms (cases 5 and 21) were underestimated in size by MR angiography owing to slight reduction of flow signals. All other aneurysms had signal as intense as the parent artery and were similar in maximum size to that seen at IA-DSA.

In case 12, MR angiography showed an aneurysm with a diameter of 4 mm at the right middle cerebral artery bifurcation, which was also shown with IA-DSA. However, we suspected that the middle cerebral artery aneurysm might be unruptured, because major hemorrhage was in the suprasellar cistern rather than in the right sylvian fissure. Neither routine MR angiography nor routine IA-DSA depicted any other aneurysm. Additional targeted MIP images, which focused on the region of the anterior communicating artery, were made during the time of IA-DSA. The targeted MIP images showed a 2-mm aneurysm arising from the anterior communicating artery and showed the direction of the aneurysm projection in relation to the parent artery. The targeted MIP images were of assistance for IA-DSA, suggesting an optimal projection angle for depicting the ruptured aneurysm (Fig 2). In case 21, routine IA-DSA images did not show any ruptured aneurysms; however, an oblique submentovertical view, based on the MR angiogram, did show a ruptured aneurysm.

In case 20, the readers prospectively pointed out an unruptured 5-mm aneurysm at the right middle cerebral artery bifurcation, but missed

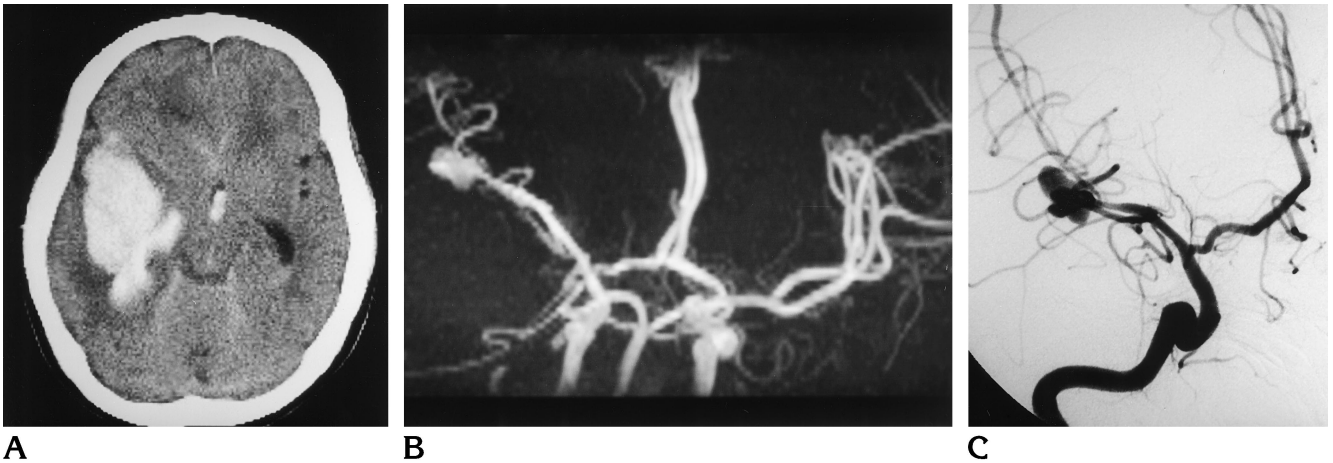

Fig 1. Case 19: 14-year-old boy with a history of acute febrile mucocutaneous lymph-node syndrome.

A, Initial CT scan shows a large subarachnoid hemorrhage and intracerebral hematoma around the right sylvian fissure.

B, MR angiogram (39/7,20/1) obtained on day 1 clearly shows an irregularly shaped 12-mm aneurysm in the distal portion of the right middle cerebral artery. No background signal from the hematoma is apparent. Upward deviation of the right middle cerebral artery due to the hematoma is noted; however, no vasospasm is seen.

C, Anteroposterior IA-DSA of the right internal carotid artery confirms a ruptured aneurysm arising from the distal portion of the right middle cerebral artery.

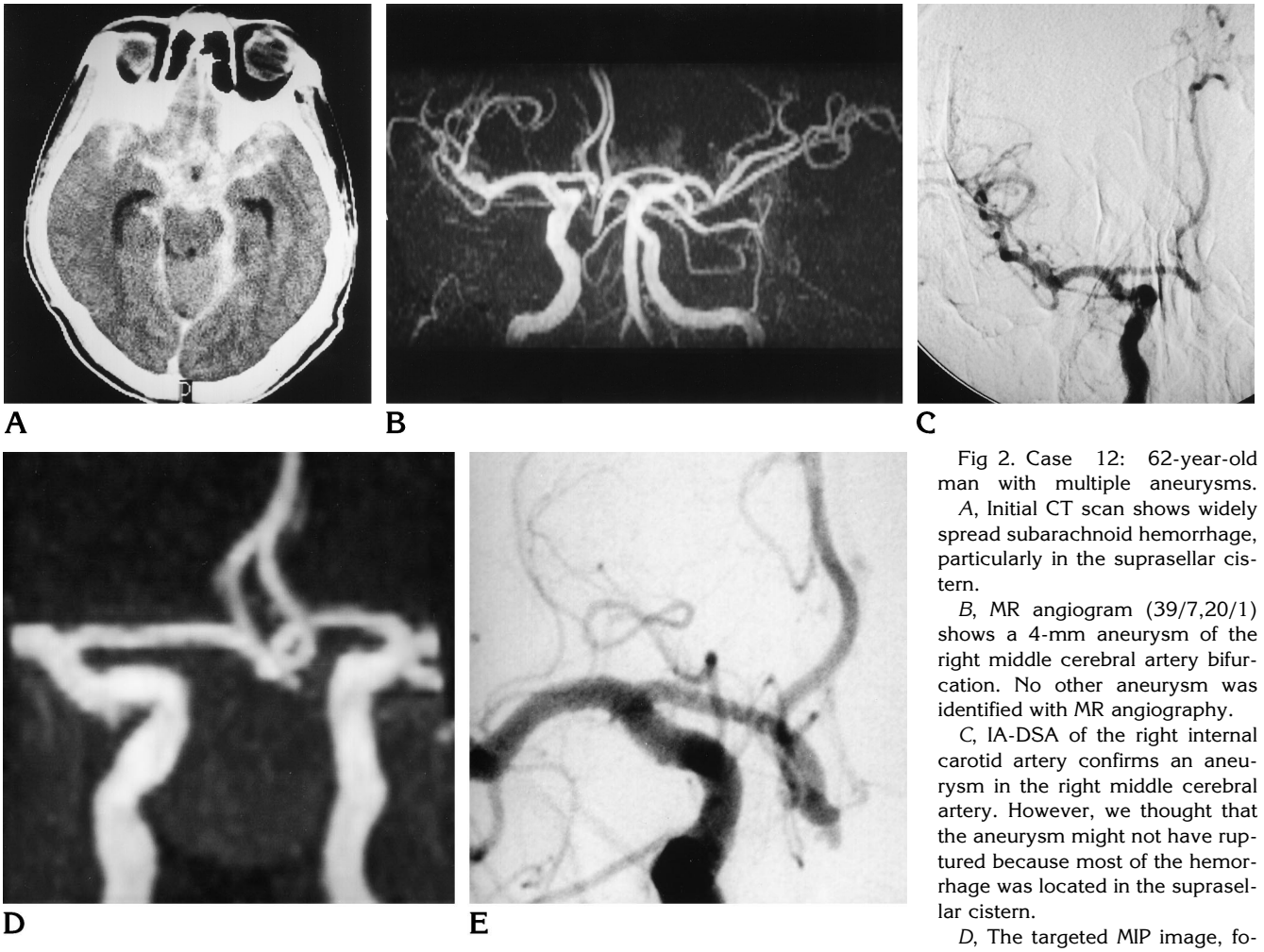

Fig 2. Case 12: 62-year-old man with multiple aneurysms.

A, Initial CT scan shows widely spread subarachnoid hemorrhage, particularly in the suprasellar cistern.

B, MR angiogram (39/7,20/1) shows a 4-mm aneurysm of the right middle cerebral artery bifurcation. No other aneurysm was identified with MR angiography.

C, IA-DSA of the right internal carotid artery confirms an aneurysm in the right middle cerebral artery. However, we thought that the aneurysm might not have ruptured because most of the hemorrhage was located in the suprasellar cistern.

D, The targeted MIP image, focused on the region of the anterior communicating artery, shows a small 2-mm aneurysm arising from the anterior communicating artery.

E, Oblique anteroposterior IA-DSA image of the internal carotid artery from the same direction as the targeted MIP image (*D*) confirms a small aneurysm in the anterior communicating artery. The aneurysm was proved to be ruptured during the operation.

another small (2-mm) ruptured aneurysm at the anterior communicating artery. The latter was detected retrospectively by MR angiography (Fig 3). In cases 21 and 22, ruptured aneurysms were identified prospectively, but other small unruptured aneurysms were not identified. Those were, however, identified retrospectively by MR angiography. In case 26, the readers could not identify a ruptured aneurysm in the distal portion of the right anterior inferior cerebellar artery, even retrospectively (Fig 4).

Discussion

Rupture of intracranial aneurysms is a major cause of subarachnoid hemorrhage. Three-dimensional TOF MR angiography is a more effective technique for detecting intracranial aneurysms than is two-dimensional TOF or 3-D phase-contrast methods (4, 5). Three-dimensional TOF MR angiography provides good spatial resolution, an acceptable acquisition time, and minimal signal loss caused by a turbulent flow. It is widely used to find unruptured aneurysms in patients who are at high risk for aneurysms (warning headaches, occulomotor palsy, and a family history) as well as in asymptomatic patients (6).

Depiction of ruptured aneurysms in patients with acute subarachnoid hemorrhage is a goal for intracranial MR angiography. However, its use in detecting aneurysms in acute subarachnoid hemorrhage is still limited, because an urgent examination is required and diagnosis of aneurysms with the use of this technique has not been satisfactory. In addition, conventional

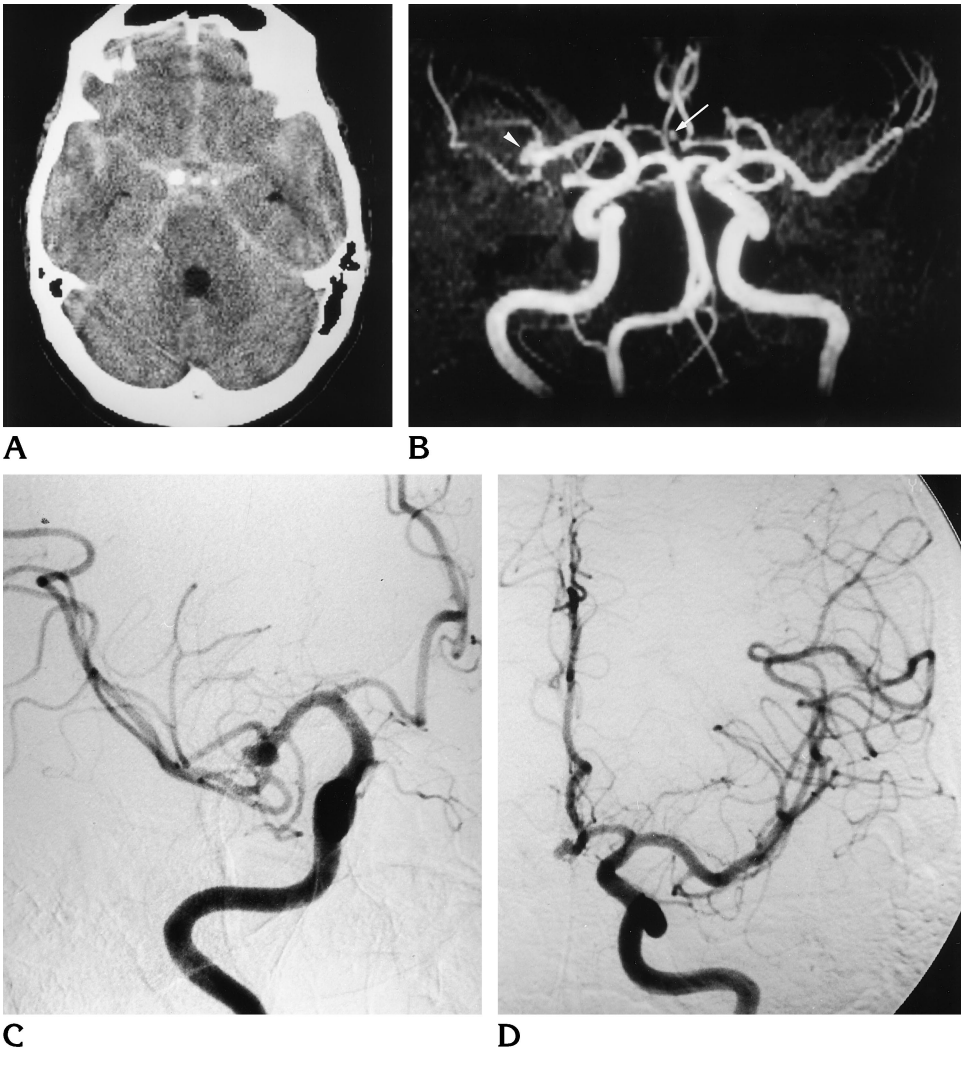

Fig 3. Case 20: 48-year-old man.

A, Initial CT scan shows widely spread subarachnoid hemorrhage.

B, MR angiogram (39/7,20/1). The readers correctly pointed out a 5-mm aneurysm at the right middle cerebral artery bifurcation (*arrowhead*); however, they prospectively missed a small 2-mm aneurysm of the anterior communicating artery (*arrow*).

C and *D*, IA-DSA of both internal carotid arteries clearly shows aneurysms of both the right middle cerebral artery and the anterior communicating artery. The latter was confirmed at surgery to be a ruptured aneurysm causing the subarachnoid hemorrhage.

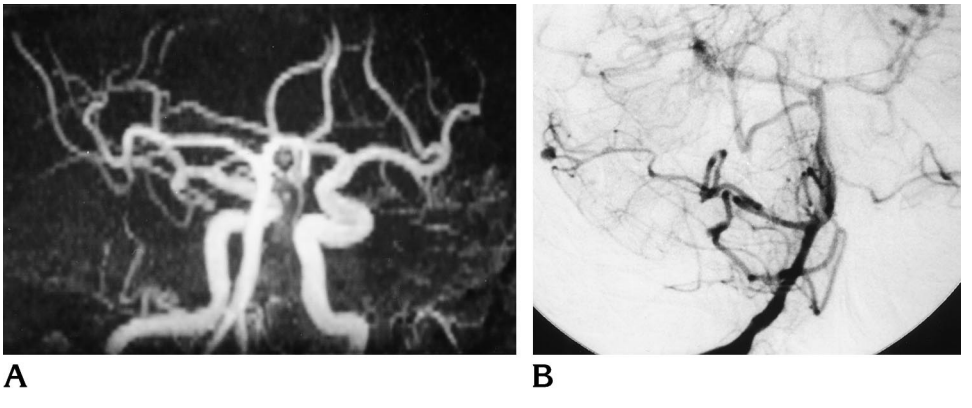

Fig 4. Case 26: 75-year-old woman.

A, MR angiogram (39/7,20/1) does not depict any ruptured aneurysm.

B, IA-DSA of the vertebral artery shows a small aneurysm located in the distal portion of the right anterior inferior cerebellar artery.

angiography can detect vascular spasm while MR angiography usually cannot. Generally, patients with acute subarachnoid hemorrhage are examined by conventional angiography to search for ruptured aneurysms and/or arteriovenous malformations. We are aware of one report on the prospective use of MR angiography for the detection of aneurysms in patients with acute subarachnoid hemorrhage (1).

Various factors and conditions may influence depiction of intracranial aneurysms with MR angiography in patients with subarachnoid hemorrhage. Vasospasm due to surrounding hematoma is a causative factor for poor depiction of the parent artery and ruptured aneurysms. Vasospasm usually occurs 3 to 13 days after the ictus of subarachnoid hemorrhage, and often leads to delayed ischemic syndrome and death (7). Vessel signals on 3-D TOF MR angiograms generally depend on flow velocity; this technique is insensitive to a slow or complex flow. Vasospasm could cause slow turbulent flow and, therefore, result in loss of signal intensity of aneurysms and of the parent artery because of phase dispersion. In this study, however, all but two patients had intense signals in ruptured aneurysms. In these two patients (cases 5 and 21), the diagnosis was made by a partial signal loss in the ruptured aneurysms. However, no patient had vasospasm, and, accordingly, "excellent" images were obtained. MR examinations should be performed in the early stage of subarachnoid hemorrhage, before vasospasm occurs.

Signal changes of paramagnetic blood-breakdown products affect the visibility of ruptured aneurysms, particularly in cases of complicated intraparenchymal hemorrhage. Conversion of oxyhemoglobin to methemoglobin in the subarachnoid space tends to be delayed because of the high oxygen tension in the cerebrospinal fluid compared with the parenchymal component of the brain. Methemoglobin shows high signal intensity during 3D-TOF sequences for MR angiography (T1-shortening effect) and obscures signals from vessels and aneurysms (8). All patients in this study underwent MR angiography in the acute stage (day 1 or 2); therefore, blood was still hypointense relative to flow signals in the aneurysm.

An imaged volume of MR angiography is limited and a saturation effect leads to signal loss in vessels deep in the slab. Multislab acquisition methods are effective for obtaining a large imaged volume and for reducing a saturation effect in the slab. However, we do not use a multislab method routinely because it requires a longer acquisition time. In the emergency setting, it is essential to minimize the examination time. The minimum section thickness allowed in the 3-D FISP sequence implemented on our MR system is 0.82 mm; however, a 1.0-mm section thickness was adopted for every patient so as to obtain a larger imaged volume within a reasonable acquisition time. The TONE technique is also helpful for suppressing progressive saturation of spins deep within a slab. The MTS suppresses signal from stationary tissue and enhances flow signals of intracranial arteries.

Patients with acute subarachnoid hemorrhage are often critically ill and uncooperative because of altered consciousness and neurologic deficits. Rehemorrhage from a ruptured aneurysm is a significant and severe complication in the acute stage, increasing the likelihood of death. Thus, critically ill patients were excluded from this study.

Appropriate sedation was administered before the MR study, and oxygen was titrated for the patients. Radiologists and neurosurgeons watched the patients carefully during the MR examinations from the control room or, when necessary, adjacent to the patients in the examination room. No significant complications occurred during or after MR angiography in any patients in this study.

We believe that the overall accuracy in the detection of ruptured aneurysms in this study was satisfactory, since 35 (90%) of 39 aneurysms were identified on an emergency basis with MR angiography. At least one aneurysm was identified via MR angiography in 25 (96%) of 26 patients with aneurysms proved by IA-DSA. There was only one false-negative outcome (case 26), which was due to a distal aneurysm beyond the accuracy limit of current MR angiography (Fig 4). In effect, high-resolution MR angiography is a helpful diagnostic technique for identifying ruptured aneurysms, even in patients with acute subarachnoid hemorrhage.

Conventional angiography is still needed for preoperative planning of intracranial aneurysms, since this technique accurately shows overall aneurysmal anatomy (eg, the relationship to the parent artery and surrounding perforators, width of neck, and presence of a bleb). However, MR angiography offers many advan-

tages over conventional angiography for the depiction of ruptured aneurysms. MR angiography can be performed within about 20 minutes, including the time for patient preparation, data acquisition, MIP calculation, and diagnosis. It can also be applied to patients with renal dysfunction (case 10) or a history of severe allergy to iodine-based contrast agents.

MR angiography conveys precise anatomic information on ruptured aneurysms, which is sometimes better than conventional angiography. Multiple-projection images can be reconstructed from one 3-D volume data set. Stereoscopic observation from multiple directions and targeted MIP images are helpful for avoiding an overlap between an aneurysm and adjacent arteries, and clearly show the direction of an aneurysm projection in relation to the parent artery (case 12, Fig 2; and case 21). Accordingly, an angiographer can choose the appropriate projection angle that optimally depicts aneurysms, reducing total examination time of subsequent IA-DSA. Several investigators have also reported cases in which MR angiography depicted ruptured aneurysms that were invisible by conventional angiography (9, 10).

In this study, three of the four aneurysms that were missed on prospective MR angiograms occurred in patients with multiple aneurysms or were 3 mm or less in diameter (cases 20, 21, and 22). In particular, a ruptured aneurysm was not identified prospectively in one patient with multiple aneurysms (case 20). When one aneurysm is depicted, other aneurysms might be missed (cases 20, 21, and 22); thus, it is of paramount importance to observe carefully not only the aneurysm's expected location but also other common sites of aneurysms, such as near the circle of Willis, by using targeted MIP and source images. Searches for other aneurysms need to be enforced, especially when a detected aneurysm might be unruptured (case 12, Fig 2).

Although MR angiography does not completely substitute for conventional angiography in acute subarachnoid hemorrhage, it offers helpful and reliable information on ruptured aneurysms for subsequent conventional angiography. Optimized projection angles clearly depict ruptured aneurysms in relation to the parent artery. Missed aneurysms (occult aneurysms) can be obviated by careful observation of multiple MR angiographic projections and targeted MIP images before proceeding with conventional angiography. We conclude that high-resolution MR angiography might be a useful adjunctive study to conventional angiography in patients with acute subarachnoid hemorrhage.

Acknowledgments

We thank the neurosurgeons at our hospital, including Drs Sugiyama, Doi, Iwama, Hayashi, Asamoto, Ogai, and Hino, and all the MR and angiography technical assistants in the Department of Radiology.

References

1. Anzalone N, Triulzi, Scotti G. Acute subarachnoid hemorrhage: 3D time-of-flight MR angiography versus intra-arterial digital angiography. *Neuroradiology* 1995;37:257–261
2. Stock KW, Radue EW, Jacob AL, Bao XS, Steinbrich WS. Intracranial arteries: prospective blinded comparative study of MR angiography and DSA in 50 patients. *Radiology* 1995;195:451–456
3. Hunt WE, Kosnik EJ. Timing and projective care in intracranial aneurysm surgery. *Neurosurgery* 1974;11:79–89
4. Korogi Y, Takahashi M, Mabuchi N, et al. Intracranial aneurysm: diagnostic accuracy of the three dimensional, Fourier, transform, time-of-flight MR angiography. *Radiology* 1994;193:181–186
5. Huston J III, Nichols DA, Leutner PH, et al. Blinded prospective evaluation of sensitivity of MR angiography to known intracranial aneurysms: importance of aneurysm size. *AJNR Am J Neuroradiol* 1994;15:1607–1614
6. Ronkainen A, Puranen MI, Hernesniemi JA, et al. Intracranial aneurysms: MR angiographic screening in 400 asymptomatic individuals with increased familial risk. *Radiology* 1995;195:35–40
7. Weir BKA. The effect of vasospasm on morbidity and mortality after subarachnoid hemorrhage from rupture aneurysm. In: Wilkins RH, ed. *Cerebral Arterial Spasm*. Baltimore, Md: Williams & Wilkins; 1980:385–393
8. Bradley WG Jr, Schmidt PG. Effect of methemoglobin formation on the MR appearance of subarachnoid hemorrhage. *Radiology* 1985;156:99–103
9. Curnes JT, Shogry MEG, Clarck DC, Elsner HJ. MR angiographic demonstration of an intracranial aneurysm not seen on conventional angiography. *AJNR Am J Neuroradiol* 1992;14:971–973
10. Gouliamos A, Gotsis E, Vlahos L, et al. Magnetic resonance angiography compared to intra-arterial digital subtraction angiography in patients with subarachnoid hemorrhage. *Neuroradiology* 1992;35:46–49